Journal of Applied Polymer Science

Rapid swelling and deswelling of semi-interpenetrating network poly(acrylic acid)/poly(aspartic acid) hydrogels prepared by freezing polymerization

Swee Lu Lim,[1] Willie Ngee Hon Tang,[2] Chien Wei Ooi,[1,3] Eng-Seng Chan,[1,3] Beng Ti Tey[1,3]

[1]Chemical Engineering Discipline, School of Engineering, Monash University Malaysia, Jalan Lagoon Selatan, Bandar Sunway 47500 Selangor, Malaysia

[2]Department of Chemical and Biomolecular Engineering, University of Melbourne, Victoria 3010, Australia

[3]Advanced Engineering Platform, Monash University Malaysia, Jalan Lagoon Selatan, Bandar Sunway 47500 Selangor, Malaysia

Correspondence to: B. T. Tey (E-mail: tey.beng.ti@monash.edu)

ABSTRACT: Hydrogels with semi-interpenetrating networks composed of poly(acrylic acid) (PAAc) and poly(aspartic acid) (PASP) have great potential for pharmaceutical and biomedical applications. In this study, we aimed to synthesize semi-interpenetrating PAAc/PASP hydrogels with improved swelling–deswelling properties via two-step polymerization, in which the first step of polymerization was performed at 37 °C for 15 min and the second step, the freezing polymerization, was performed at −20 °C for 24 h. The synthesized hydrogels were characterized with field emission scanning electron microscopy, Fourier transform infrared spectroscopy, and thermogravimetric analysis. The swelling and deswelling behaviors of the hydrogels in response to the ionic strength of the buffer solution were investigated. The Schott's swelling kinetic model was used to elucidate the swelling behavior of the hydrogels. The swelling and deswelling rates of the hydrogels prepared via freezing polymerization were faster than those of the hydrogels prepared via conventional polymerization. This was attributed to the large mean pore size of the freeze-polymerized hydrogels. The PAAc/PASP hydrogels that underwent freezing polymerization had better swelling–deswelling characteristics than the PAAc hydrogels. © 2016 Wiley Periodicals, Inc. J. Appl. Polym. Sci. **2016**, *133*, 43515.

KEYWORDS: crosslinking; gels; stimuli-sensitive polymers; swelling

Received 10 September 2015; accepted 4 February 2016

DOI: 10.1002/app.43515

INTRODUCTION

Hydrogels, three-dimensional networks formed by covalently crosslinked hydrophilic polymers, can accommodate a large amount of water or biological fluids while maintaining their spatial network structure.[1] A stimulus-responsive hydrogel responds to changes in environmental conditions (e.g., pH, ionic strength, temperature, light, biomolecules, electric and magnetic fields) by undergoing abrupt changes in its volume.[2–7] Ionic-strength-responsive hydrogels hold great potential in applications such as biosensors[8] and delivery systems for genes[9] and proteins[10] because they mimic the natural environment for biomolecules and ensure the stability of the biomolecules residing in their internal structure.[11] An ionic-strength-responsive hydrogel was successfully used as a glucose sensor[12] and in a reversible enzyme binding system.[11] For example, glucose in the human body can trigger the swelling of polyacrylamide hydrogels embedded with glucose oxidase because of the increasing concentration of the anionic glucose oxidase flavin adenine dinucleotide prosthetic group.[12–14] Interpenetrating polymer networks (IPN) consists of a blend of two or more polymers that are synthesized in proximity to form the cross-linked networks held together by entanglements[15] Semi-interpenetrating (semi-IPN) hydrogel is made of two types of polymers cross-linked during polymerization. A semi-IPN hydrogel retains the intrinsic properties of both polymers, and sometimes, it has enhanced properties over hydrogels made of the discrete polymer.[16] Poly(acrylic acid) (PAAc) hydrogels exhibit swelling and deswelling behaviors in response to variations in the pH or ionic strength.[17–19] However, PAAc hydrogels require hours to weeks to achieve an equilibrium state[20] because of the low porosity and the small-size pores in the hydrogel. On the other hand, poly(aspartic acid) (PASP) is an amino-acid-based polymer that possesses desirable characteristics, such as biodegradability, biocompatibility, and toxicological suitability.[16,21]

Additional Supporting Information may be found in the online version of this article

Therefore, the incorporation of PASP into a PAAc hydrogel yields a type of biodegradable semi-IPN hydrogel featuring an improved sensitivity toward the pH or ionic strength.[1,16] A semi-IPN PAAc/PASP hydrogel was synthesized through the diffusion of acrylic acid (AAc) monomers into the PASP matrix before the polymerization step. A PAAc network formed in the presence of linear PASP polymers behaved like a reptile chain entangling with the network chains.[15] Hence, most PASP polymers in semi-IPN hydrogels would be retained as they entangle and concatenate with the PAAc network.[15] One cannot separate PASP polymers from the hydrogel network without breaking the crosslinking bonds between the monomers.[15]

The widespread application of ionic-strength-responsive hydrogels in biorelated fields, for example, drug delivery and biosensors, demands a deeper understanding of the swelling properties of semi-IPN PAAc/PASP hydrogels in physiological fluids. The responsivity of the hydrogel could be improved through increases in its porosity through a freezing polymerization step during the synthesis process. The high surface-to-volume ratio in the hydrogel allows a more rapid diffusion of solute and solvent into the hydrogel; this leads to a quicker change in the hydrogel's volume. The freezing polymerization is generally conducted in a moderately frozen medium. A temperature-responsive poly(*N*-isopropyl acrylamide-*co*-acrylic acid) hydrogel prepared via freezing polymerization demonstrated an enhanced temperature responsiveness over a hydrogel synthesized via conventional polymerization.[22] In addition, a hydrogel made of poly(*N,N*-diethyl acrylamide-*co*-acrylic acid) was prepared with a two-stage polymerization in which the first stage of the polymerization was carried out at a relatively high temperature for 15 min and the second stage, a freezing polymerization, was carried out at −30 °C for 12 h.[23] The higher temperature used in the first stage of polymerization was, the better the responsiveness of the hydrogels to stimuli such as temperature and pH was.[23] Thus, freezing polymerization has been viewed as a promising technique for producing polyelectrolyte hydrogels.

In view of the potential use of semi-IPN PAAc/PASP hydrogels in the biomedical field as biosensing materials and polymeric drug carriers/adsorbents, it is necessary to investigate the swelling kinetics of semi-IPN PAAc/PASP hydrogels in buffered saline solutions prepared at different ionic strengths. In this article, we report a method for synthesizing semi-IPN hydrogels with an expanded network structure by the two-step polymerization, wherein the initial polymerization was carried out at 37 °C for 15 min. This was followed by a freezing polymerization at −20 °C for 24 h. The swelling of the semi-IPN PAAc/PASP hydrogel was mainly ascribed to the functional groups of ionic carboxylate and nonionic carboxamide. The ionic groups were more solvated compared to the nonionic groups in the aqueous medium. The superabsorbency might have resulted from the expanded network of the hydrogel; this was attributed to the strong electrostatic repulsion force from PAAc and PASP carboxylate anions (—COO^-). The effect of the freezing polymerization on the resulting semi-IPN hydrogels was evaluated. The responsivity of the semi-IPN hydrogels to the ionic strength of phosphate-buffered saline (PBS) solution was investigated through analysis of the swelling kinetics of the hydrogels. This smart and responsive hydrogel is a promising material for building biological systems applied in the fields of biomedicine, biosensors and pharmaceuticals.

EXPERIMENTAL

Materials

PASP (molecular weight = 2000–11,000 g/mol), AAc, ammonium persulfate (APS), *N,N′*-methylene bisacrylamide (MBA), and *N,N,N′,N′*-tetramethylethylenediamine (TEMED) were purchased from Sigma-Aldrich. All of the chemicals were of analytical grade and were used without further purification.

Synthesis of the Hydrogels

The hydrogels were synthesized with free-radical polymerization (see Figure 1). According to the compositions of the hydrogels shown in Table I, AAc, PASP, APS, MBA, and TEMED were mixed into the PBS solution (700 μL, 0.02 *M*, pH 7.4) under stirring conditions. APS functioned as an initiator, whereas MBA and TEMED were used as the crosslinker and accelerator, respectively. The reaction glass vials were then incubated at 37 °C for 15 min to begin the first-step polymerization.[23,24] The conversion of the monomer in the first-step polymerization was consistent for all of the hydrogels because the synthesis conditions (concentrations of monomer and initiators, reaction time, and temperature) were kept constant. Next, we initiated the second-step polymerization by transferring the reactants immediately to a −20 °C reactor (freeze polymerization) or by incubating the reactants at 25 °C. The second-step polymerization lasted for 24 h. The synthesized hydrogels were immersed in a PBS solution (0.02 *M*, pH 7.4) for 5 consecutive days, with the PBS solution being replaced routinely to remove the unreacted AAc, PASP, and other soluble chemicals from the hydrogels. The thoroughly washed hydrogels were incubated further in the PBS solution for 7 days. No sign of leakage was observed for the synthesized semi-IPN PAAc/PASP hydrogel (see Supporting Information). Last, the hydrogels were cut into discs with a thickness of 3–4 mm and a diameter of 1 cm.

Characterization of the PAAc and Semi-IPN PAAc/PASP Hydrogels

Scanning Electron Microscopy. The interior morphology of the hydrogels was studied with field emission scanning electron microscopy (FESEM; Hitachi SU8010, Germany). The hydrogels were equilibrated in PBS solution (0.05 *M*, pH 7.4) before they were subjected to freeze drying at −109 °C *in vacuo*. Before they were viewed under FESEM, the dried hydrogels were sputter-coated with platinum.

Fourier Transform Infrared (FTIR) Spectroscopy. The hydrogels were dried until a constant weight was obtained. The dried hydrogels were then ground into a fine powder, which was then compressed into a disc form. The pelleted samples were analyzed with an FTIR spectrometer (Thermo Scientific Nicolet iS10, USA) in the region 4000–550 cm^{-1}.

Thermogravimetric Analysis. Thermogravimetric analysis of the dried hydrogels was conducted with a thermogravimetric analyzer (model Q50, TA Instruments, USA). The thermograms

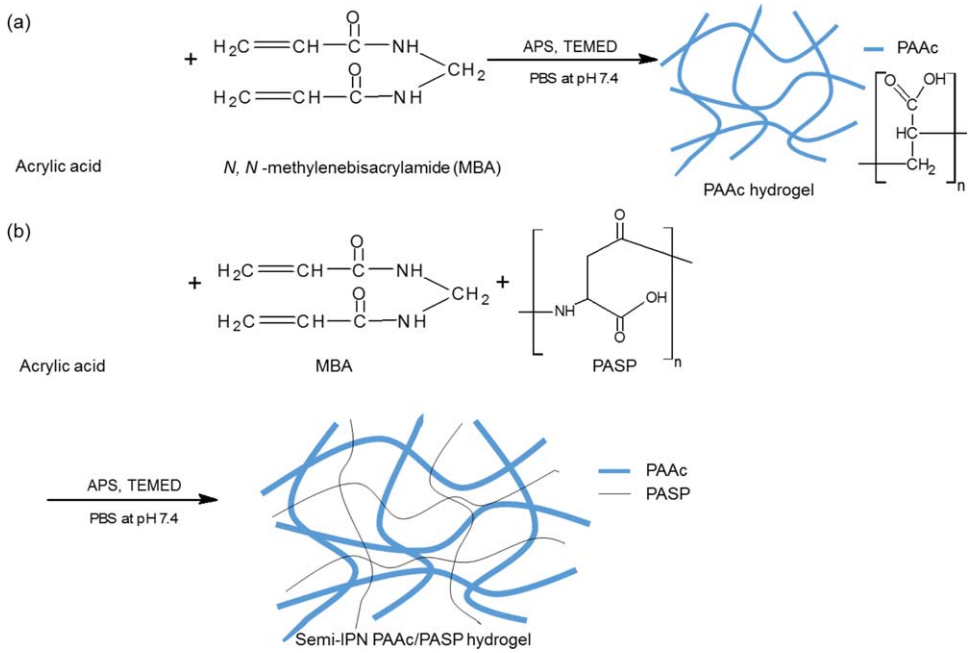

Figure 1. Synthesis steps of the (a) PAAc and (b) semi-IPN PAAc/PASP hydrogels. [Color figure can be viewed in the online issue, which is available at wileyonlinelibrary.com.]

of the hydrogels were recorded at a heating rate of 10 °C/min over the temperature range 10–600 °C. During the analysis, nitrogen gas was purged at a flow rate of 20 mL/min.[21] $t_{1/2}$ was calculated as the temperature at which half the composition was degraded.[25]

Equilibrium Swelling Ratio (S_{eq}) of the Hydrogels

We investigated S_{eq} of the hydrogel by allowing the hydrogel to swell in PBS solution (0.05 *M*, pH 7.4) for 24 h at room temperature. The wet hydrogel was then weighed. S_{eq} (g/g) was calculated with eq. (1)[1]:

$$S_{eq} = (W_{eq} - W_d)/W_d \quad (1)$$

where W_{eq} is the weight the of the equilibrium-swollen hydrogel (g) and W_d is the weight of the dried hydrogel (g).

Swelling Behavior of the Hydrogels

The swelling behavior of the hydrogel in the simulated physiological fluids was investigated with PBS solutions (pH 7.4) prepared at different ionic strengths (0.05 and 0.15 *M*). The classical gravimetric method was used to determine the swelling characteristics of the hydrogels. Briefly, the hydrogels were first pre-equilibrated in a 0.15 *M* PBS solution. Subsequently, the hydrogels were transferred into a 0.05 *M* PBS solution and incubated at room temperature until they reached the equilibrium state. After we blotted excess water on the hydrogel surface, we measured the weights of the hydrogels. Each measurement of sample weight was repeated three times.

The swelling ratio of the hydrogel at time t (S_t) was determined with the following eq. (2)[1]:

$$S_t(g/g) = (W_t - W_d)/W_d \quad (2)$$

where W_t is the weight of swollen hydrogel at time t (g).

Table I. Feed Compositions and Polymerization Conditions for the Preparation of the PAAc and Semi-IPN PAAc/PASP Hydrogels

						First-step polymerization		Second-step polymerization	
Sample code	AAc (mmol)	PASP (mmol)	APS (mg)	MBA (mg)	TEMED (μL)	Temperature (°C)	Time (min)	Temperature (°C)	Time (h)
PAA 37-25	1	0	2	1	40	37	15	25	24
PAA 37-F20	1	0	2	1	40	37	15	−20	24
IPN 37-25	1	0.01	2	1	40	37	15	25	24
IPN 37-F20	1	0.01	2	1	40	37	15	−20	24
SC	1	0	2	1	40	25	15	25	24

AAc, PASP, APS, MBA, and TEMED were dissolved in 700 μL of PBS. The synthesized hydrogels are named according to the type of hydrogel formed and the reaction temperature of the first- and second-step polymerizations. In the sample codes, "PAA" and "IPN" refer to the PAAc hydrogel and the semi-IPN PAAc/PASP hydrogel, respectively. The PAAc hydrogel prepared via the conventional method was denoted as "SC".

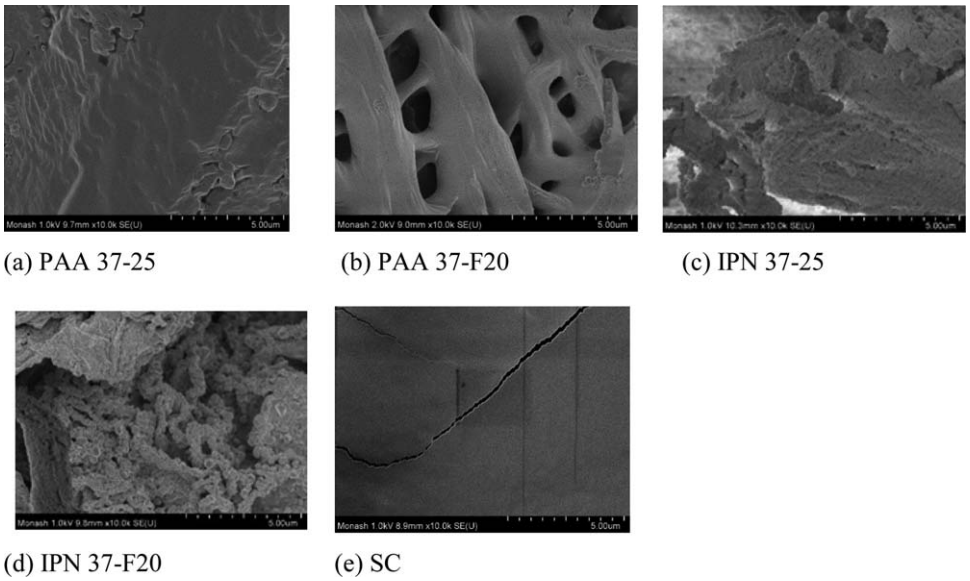

Figure 2. Cross-sectional FESEM images of the hydrogels.

Swelling Kinetics of the Hydrogels. S_t was fitted into the following Schott's second-order swelling kinetics model [eq. (3)][26] to obtain the swelling kinetic parameters of the hydrogels[1,27]:

$$dS/dt = k_s(S_{eq} - S_t)^2 \quad (3)$$

where S is defined as the swelling of hydrogel or solvent uptake by hydrogel at time t and k_s is the rate constant [g of gel (g of water)$^{-1}$ min^{-1}].

By applying the initial conditions, that is, $S_t = 0$ at $t = 0$ and $S_t = S_t$ at $t = t$, we integrated the second-order kinetics equation into the following equation [eq. (4)][1]:

$$t/S_t = (1/r_0) + (1/S_{eq})t \quad (4)$$

where r_0 is the initial swelling rate [g of water (g of gel)$^{-1}$ min^{-1}] and is equivalent to $1/k_s S_{eq}^2$.[27–29]

Deswelling Kinetics of the Hydrogels

The pre-equilibrated (in PBS solution at 0.05 *M* and pH 7.4) hydrogel was transferred to a PBS solution (0.15 *M*, pH 7.4). The wet weight of the hydrogel at different time t (W_t) was measured after the removal of excess water from the hydrogel surface. The water retention percentage (WR %) of the hydrogel was calculated with eq. (5)[21]:

$$\text{WR } \% = (W_t - W_d)/(W_{eq} - W_d) \times 100\% \quad (5)$$

Oscillating Swelling–Deswelling Kinetics of the Hydrogels

The hydrogels were pre-equilibrated in PBS solution (0.15 *M*, pH 7.4) at room temperature for 24 h. The oscillatory swelling–deswelling of the hydrogels in PBS (pH 7.4) solutions at alternate ionic strengths of 0.05 and 0.15 *M* was examined. In brief, after the hydrogel was incubated in 0.05 *M* PBS solution for 40 min, the swollen hydrogel was transferred to the 0.15 *M* PBS solution for the next 40-min incubation. This 80-min swelling–deswelling cycle was repeated twice, and the wet weight of the hydrogel was recorded.[21] S_t was calculated with eq. (2).

RESULTS AND DISCUSSION

FESEM Analysis

The microstructure of the hydrogels might have been related to the diffusion pattern of water in the hydrogels. The micrographs showing the interior morphologies of the freeze-dried hydrogels are presented in Figure 2(a–e). The surfaces of the PAAc hydrogels [Figure 2(a,b)] were smoother than those of the IPN hydrogels [Figure 2(c,d)]. The rough and porous surfaces of the IPN hydrogel was attributed to the presence of PASP in its structure. The PASP contained hydrophilic groups (—CONH and —COOH) that were ionized (—COO$^-$) during the polymerization process. The repulsive forces among the PASP's carboxylate anions[30] resulted in the formation of a porous gel and rendered a highly expanded network in the IPN hydrogel structure. The presence of a void or inhomogeneity in the hydrogel was caused by the microphase separation between the AAc monomers and PASP polymer chains; this created a domain difference followed by crosslinking to form the polymer network.[31] The hydrogel network upheld the spatial arrangement and conformation history of its porous structure.[32–34] Hence, an expanded network structure with a porous molecular conformation was retained even after the hydrogel was freeze-dried. The micrographs of the hydrogels affirmed that the porous structure resulted from the expanded network of the hydrogel.

As shown in Figure 2(b,d), the microstructures of the hydrogels formed via the second-step freezing polymerization (i.e., PAA 37–F20 and IPN 37–F20) were more open/loose, and they contained larger pores in comparison to their respective types formed at 25 °C in the second polymerization step [see Figure 2(a,c)]. The freezing polymerization facilitated the expansion of the hydrogel network and gave the large-pore microstructure of the hydrogel. This phenomenon might have been due to the formation of crystallized water molecules, which acted as pore-forming agents in the hydrogel structure, during the freezing polymerization.[23,35] On the contrary, the cross-sectional views of PAA 37–25 and the conventionally polymerized PAAc

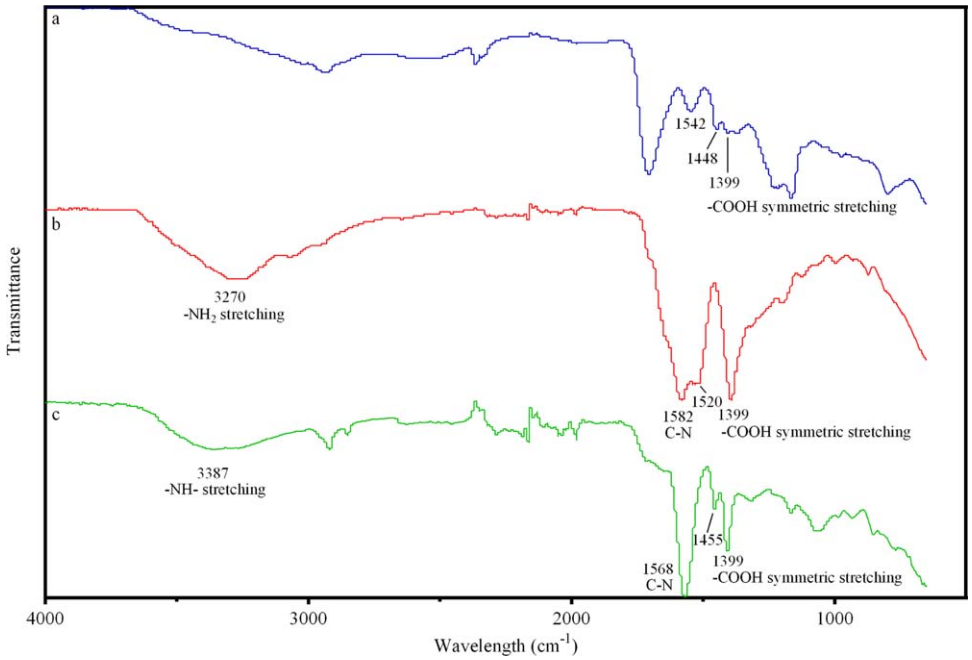

Figure 3. FTIR spectra of the (a) PAAc, (b) PASP, and (c) semi-IPN PAAc/PASP hydrogels. [Color figure can be viewed in the online issue, which is available at wileyonlinelibrary.com.]

hydrogel (SC) showed the nonporous surfaces [Figure 2(a,e)]. Microsize particles were found in IPN 37–F20 [Figure 2(d)]. These particles were believed to be the small-size gels synthesized during the two-step polymerization.[23]

FTIR Spectrum of the PAA/PASP Semi-IPN Hydrogel

The chemical composition of the PAA/PASP semi-IPN hydrogel was studied by the FTIR analysis. The FTIR spectra of the PAAc, PASP, and semi-IPN PAAc/PASP hydrogel are shown in Figure 3. PASP contained carboxylic acid groups (—COOH), as evidenced by the peak at 1399 cm^{-1}, which corresponded to the symmetric stretching vibrations of carboxylate groups. As expected, a sharp peak at 1399 cm^{-1} was found in the FTIR spectrum of the semi-IPN PAAc/PASP hydrogel [Figure 3(c)]. The peaks at 1520 and 1582 cm^{-1} in the FTIR spectrum of PASP [Figure 3(b)] indicated the amide group in PASP. A strong peak associated with the amide group was also found at 1568 cm^{-1} in the FTIR spectrum of the semi-IPN PAAc/PASP hydrogel [Figure 3(c)]. These results confirm the presence of PASP in the semi-IPN PAAc/PASP hydrogel. On the other hand, the broad bands at about 3270 cm^{-1} in the FTIR spectra of the PASP [Figure 3(b)] and semi-IPN PAAc/PASP hydrogel [Figure 3(c)] represented the stretching bands of the —NH_2 group, whereas the peak at 3387 cm^{-1} was attributed to the —NH stretching vibrations of PASP in the semi-IPN PAAc/PASP hydrogel. None of these bands were noted in the FTIR spectrum of PAA [Figure 3(a)]; this verified the incorporation of PASP in the semi-IPN PAAc/PASP hydrogel structure.

Thermal Analysis

Thermogravimetric analysis tracings of the PAAc and semi-IPN PAAc/PASP hydrogels are depicted in Figure 4. The weight loss in the hydrogel was mainly caused by the thermal decomposition of the polymer and the splitting of the polymer chain. The hydrogels underwent three stages of thermal decomposition. In the first stage of decomposition, the weight losses in the semi-IPN PAAc/PASP hydrogels (IPN 37–25 and IPN 37–F20) and PAAc hydrogels (SC, PAA 37–25, and PAA 37–F20) were 17 and 13%, respectively. The weight losses in the hydrogels at this stage were mainly associated with the loss of moisture content from the hydrogels. Beyond this stage, the splitting and breaking of the main polymer chains in the hydrogels occurred, and the most intensive decomposition began at 340 °C. The major decomposition of the hydrogel took place in the second stage of thermal decomposition (220–340 °C), whereas the maximum decomposition occurred in the third stage of thermal decomposition (340–440 °C). The residual mass percentages of the PAAc and semi-IPN PAAc/PASP hydrogels were about 10 and 30%, respectively. $t_{1/2}$ of the semi-IPN PAAc/PASP hydrogel (381 °C)

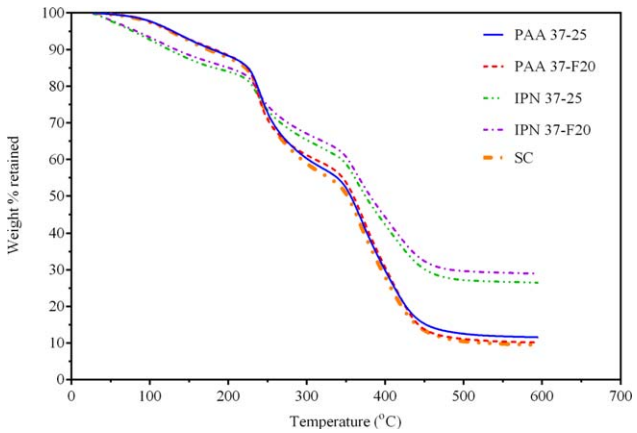

Figure 4. Thermogravimetric analysis of the SC, PAAc, and semi-IPN PAAc/PASP hydrogels. [Color figure can be viewed in the online issue, which is available at wileyonlinelibrary.com.]

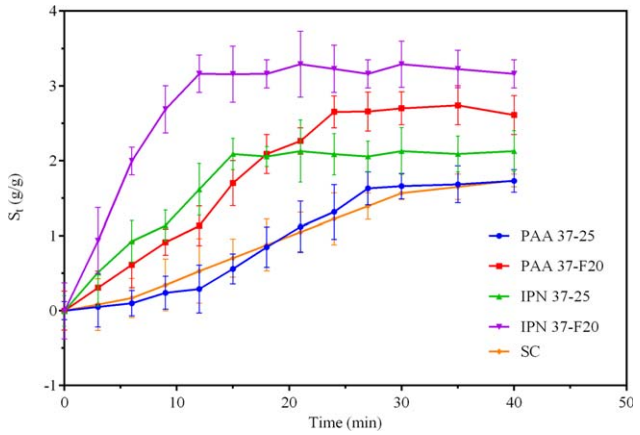

Figure 5. Swelling kinetics of the hydrogels incubated in a 0.05 *M* PBS solution (pH 7.4). The hydrogels were first equilibrated in a 0.15 *M* PBS solution (pH 7.4) for 24 h. [Color figure can be viewed in the online issue, which is available at wileyonlinelibrary.com.]

was higher than that of the PAAc hydrogel (355 °C). These results demonstrate that the thermal stability of the semi-IPN PAAc/PASP hydrogel was greatly enhanced by the incorporation of PASP into the PAAc hydrogels. This was attributed to the good thermal stability and high thermal resistance of PASP.

Swelling Kinetics of the Hydrogels

Figure 5 depicts the swelling kinetics of the hydrogels. All of the hydrogels exhibited swelling tendencies shortly after they were immersed in the 0.05 *M* PBS solution. The hydrogel swelling was reliant on the solvent diffusion and polymer network relaxation.[36] Upon the transfer of the hydrogel from the 0.15 *M* PBS solution to the 0.05 *M* PBS solution, the difference in the mobile ion concentration between the interior of the hydrogel and the environmental solution increased. Water molecules migrated into the dynamically formed spaces between polymer chains. This phenomenon was ascribed to an increase in the osmotic pressure of the hydrogels. The imbalance in osmotic pressure led to the flushing of water molecules. Consequently, the ion gradient was compensated by the swelling of the hydrogel.

The second-order swelling kinetics model[26] was used to analyze the swelling kinetics of the hydrogels. Empirically, the swelling kinetics fit perfectly with the second-order rate equation, as given in eq. (3). The swelling kinetics at any predetermined time t could be expressed by S_t of the hydrogel; this was the water uptake of the hydrogel from its surroundings. A linear correlation between t/S_t and t was obtained upon the integration of eq. (3). Figure 6 was plotted on the basis of eq. (4), where $S_{eq(calc)}$ and k_s were obtained from the slope and intercept, respectively, of the linear regression.

The calculated swelling kinetics parameters and the statistical parameters of these fittings are depicted in Table II. A good fitting of the experimental swelling data to Schott's swelling kinetics expression[26,37] was indicated by a high regression coefficient ($R^2 = 0.9994$–1), a low χ^2 value (i.e., 0.002625–0.01403), and a high-regression F value (i.e., 18,875–251,983) of the fittings. Furthermore, the $S_{eq(calc)}$ values of the hydrogels were found to be very close to the $S_{eq(exp)}$ values. These results confirmed that the ionic-strength responsiveness of the hydrogel perfectly obeyed the second-order rate expression by Schott.[26]

The relaxation rate of the polymer network was highly dependent on the properties of the hydrogel, including the rigidity, hydrophilicity, crosslinking density, dimension, and proportion of amorphous region in the hydrogel.[27] The presence of PASP in the semi-IPN hydrogel increased the overall number of ionized hydrophilic —COOH groups in the hydrogel. As shown in Figure 5 and Table II, the incorporation of PASP into the PAAc hydrogel structure significantly improved the swelling and deswelling rates of the hydrogels. IPN 37–25 showed at least a twofold increase in both k_s and r_0 over the values of PAA 37–25.

The electrostatic repulsion force was strongly associated with the proportion of attached ionizable groups in the hydrogel.[16] The synthesized semi-IPN PAAc/PASP hydrogels were responsive to pH changes. At pH 7.4, the pendant carboxylic acid (—COOH) and ammonium ions ($—NH^{3+}$) in the hydrogel were deprotonated into carboxylic ions ($—COO^-$) and amine groups ($—NH_2$), respectively. The electrostatic repulsion force occurring within the hydrogel were mainly attributed to the anionic carboxylic ions, which were the dominant repulsion force that induced the swelling of the hydrogel. The enhanced electrostatic repulsion led to a higher porosity in the hydrogel; this was reaffirmed by the FESEM results [Figure 2(c,d)]. The microstructure pores in the semi-IPN PAAc/PASP hydrogel acted as hydrophilic microchannels that accelerated the diffusion of water molecules from the PBS solution into the hydrogel; this enhanced the responsiveness of the hydrogel. Hence, we concluded that the number of charged groups within the hydrogel and the hydrophilicity of the hydrogel played an important role in its swelling kinetics (Table II). Overall, the ionic-strength sensitivity of the semi-IPN PAAc/PASP hydrogel was improved with the presence of PASP.

As shown in Figure 5, the freeze-polymerized hydrogels (i.e., PAA 37–F20 and IPN 37–F20) exhibited faster swelling rates in

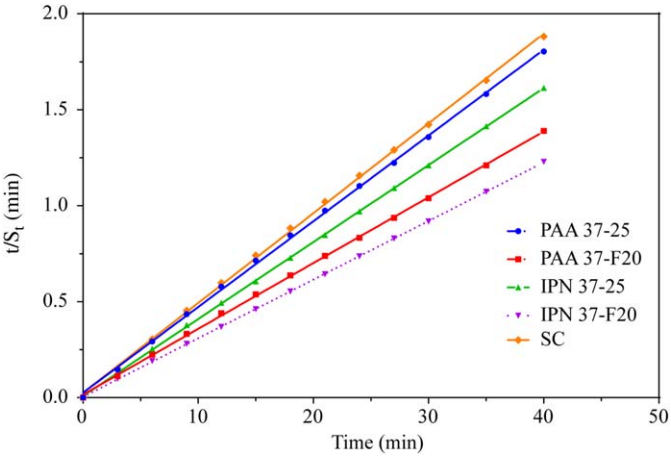

Figure 6. Linear regression of the swelling isotherms for the hydrogels in response to the changes in the ionic strength of the PBS solution. The swelling data were fitted with eq. (4). [Color figure can be viewed in the online issue, which is available at wileyonlinelibrary.com.]

Table II. Parameters of the Swelling Kinetics of the Hydrogels

Sample code	k_s (g of gel/g of water min)	r_0 (g of water/g of gel min)	$S_{eq(exp)}$ (g/g)	$S_{eq(calc)}$ (g/g)	R^2	χ^2	F
PAA 37-25	0.079	39.34	22.17	22.38	0.9994	0.01403	18,875
PAA 37-F20	0.075	63.98	28.78	29.17	0.9997	0.00802	33,949
IPN 37-25	0.189	117.30	24.78	24.93	0.9999	0.00467	137,419
IPN 37-F20	0.246	263.44	32.54	32.72	0.9999	0.00263	251,983
SC	0.087	39.65	21.26	21.37	0.9995	0.01363	21,918

$S_{eq(exp)}$ is the equilibrium swelling ratio calculated using eq. 1, whereas $S_{eq(calc)}$ is equilibrium swelling ratio obtained from the slope value of the linear regression in Figure 6. Chi-square (χ^2) and F statistical tests were calculated to evaluate the validity of the kinetic model.

response to the external ionic-strength changes than those prepared at room temperature (i.e., PAA 37–25 and IPN 37–25, respectively). On the basis of the results shown in Table II, the freezing polymerization greatly improved r_0 of the hydrogel but exerted a minimal influence on k_s. After the first-step polymerization, mobile water molecules diffused into the partially formed hydrogel before freezing at −20 °C. Before the freezing step (at −20 °C), the free water molecules diffused into the partially formed hydrogel during the first-step polymerization.[38] The water molecules started to crystallize at the freezing temperature. The gel-forming solution containing the reactive monomers, crosslinker, initiator, and accelerator was polymerized to form the hydrogel, whereas the void space filled with ice crystals formed the pores after thawing; thereby, a polymer network with a more open channel structure was synthesized.[38] Because the volume requirement of the crystallized water molecules was larger than that in its liquid state,[38] the mean pore size of the hydrogels prepared by the freezing polymerization was increased. This result was reaffirmed by the FESEM images (Figure 2). The surface-to-volume ratio of the hydrogel was increased because of its large and interconnected porous structure.[38] The crystallized water molecules present in the hydrogel during the polymerization rendered a highly porous structure of the hydrogel; this enhanced the hydrogel's water absorbency and swelling capability. On the contrary, the dense and less porous structures found in PAA 37–25 and SC highly resisted the diffusion of water molecules into the hydrogels; this explained their low response rates toward the ionic strength of the solution. One could envisage that a higher porosity would result in a rapid response rate because of the larger mesh size between the polymer chains in the hydrogel network. The larger mesh size enables the diffusions of the solute and solvent more rapidly through the hydrogel.

Deswelling Kinetics of the Hydrogels

We investigated the deswelling kinetics of the PAAc and semi-IPN PAAc/PASP hydrogels by allowing the hydrogel to deswell in a buffer having a higher ionic strength. Overall, as shown in Figure 7, the water content of the hydrogels decreased with an increase in the ionic strength of the PBS solution at pH 7.4. The diffusion of water molecules into the hydrogels was kinetically limited by the ion gradient. This was ascribed to a decrease in the osmotic pressure of the hydrogels, which was caused by the increase in the ionic strength. Consequently, the difference in the mobile ion concentrations between the interior of the hydrogel and the environmental bath was compensated for by the decrease in the swelling of the hydrogel.

Similar to the swelling behavior, the ability of the hydrogel to retain water was significantly dependent on the chemical composition of the hydrogels. The ability of hydrogels to retain water was found to be in decreasing order as follows: IPN 37–F20 > IPN 37–25 > PAA 37–F20 > PAA 37–25. This trend was in agreement with the overall number of anionic hydrophilic COOH groups present in the hydrogel. As mentioned earlier, the porous structure of the hydrogel and the hydrophilicity of the incorporated PASP were responsible for the formation of water-liberating microchannels in the semi-IPN PAAc/PASP hydrogel network.[39]

The results shown in Figure 7 demonstrate that the freeze-polymerized hydrogels (i.e., PAA 37–F20 and IPN 37–F20, respectively) possessed faster deswelling than the conventionally polymerized hydrogels (i.e., PAA 37–25 and IPN 37–25, respectively). The higher surface-to-volume ratios of the freeze-polymerized hydrogels accelerated the water diffusion.[38] Furthermore, the larger pore size in the freeze-polymerized hydrogels (i.e., PAA 37–F20 and IPN 37–F20) allowed the freed water to diffuse out quickly, and this resulted in the faster deswelling of the hydrogels.

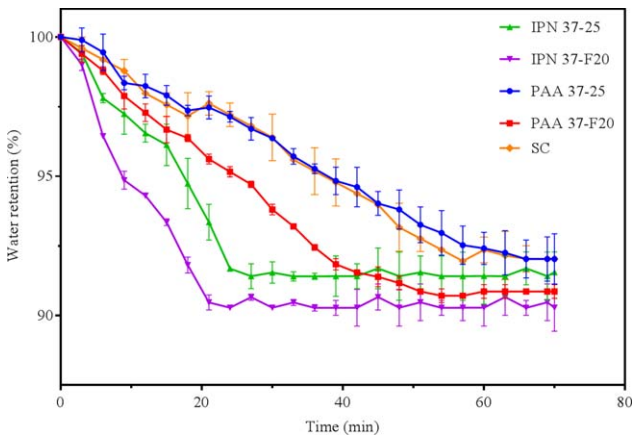

Figure 7. Deswelling kinetics of the hydrogels incubated in a 0.15 *M* PBS solution (pH 7.4). The hydrogels were pre-equilibrated in a 0.05 *M* PBS solution (pH 7.4) for 24 h. [Color figure can be viewed in the online issue, which is available at wileyonlinelibrary.com.]

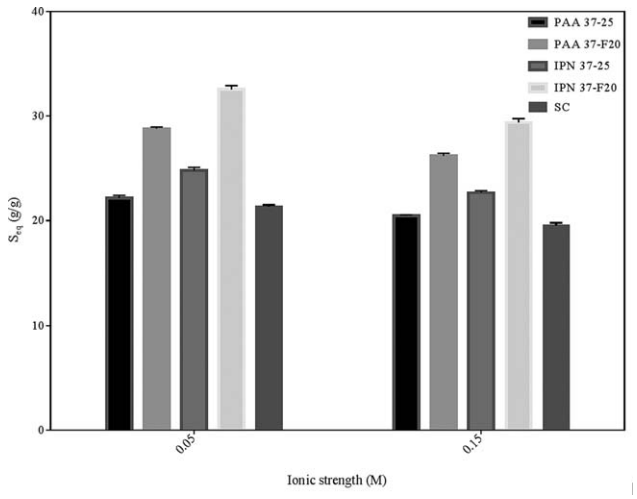

Figure 8. S_{eq} values of the hydrogels in PBS solutions (pH 7.4) prepared at different ionic strengths.

PAA 37–25 and SC exhibited the slowest rate of deswelling. The glassy and rigid layers found in them [Figure 2(a,e)] were responsible for their high resistances for water diffusion. On the contrary, IPN 37–F20 had the fastest rate of deswelling and a high rate of water diffusion because of its large mean pore size and high porosity.

Overall, SC and PAA 37–25 exhibited similar patterns of swelling (Figure 5) and deswelling (Figure 7); this indicated that the high temperature (37 °C) used in the first-step polymerization solely accelerated the polymerization process, as reaffirmed by their similar nonporous microstructures (Figure 2).

Ionic-Strength Dependence of the S_{eq} Values of the Hydrogels

The S_{eq} values of the PAAc and semi-IPN PAAc/PASP hydrogels were investigated with 0.05 and 0.15 *M* PBS solutions at pH 7.4. As shown in Figure 8, the semi-IPN PAAc/PASP hydrogels had at least a 1.13-fold increase in S_{eq} compared to their respective PAAc hydrogels. This may have been due to the increased number of hydrophilic anionic carboxylate functional groups (COO^-) in the semi-IPN PAAc/PASP hydrogel. The increase in the electrostatic repulsion force was believed to contribute the highly expanded structure in the hydrogel; this led to a higher S_{eq} value, as shown in Table II.

The S_{eq} of the freeze-polymerized PAAc hydrogel (PAA 37–F20) was at least 1.28 times higher than that of SC. This was mainly attributed to the pore formation during freezing polymerization. The pore size and porosity of the hydrogel played an important role in the S_{eq} values of the hydrogels. During the swelling process, the preformed pores inside the polymer network were rapidly filled with the water molecules. Meanwhile, the ability of the polymer chains to attract water molecules from the surroundings depended on the attractive force between the water molecules and the polymer's functional groups, particularly carboxylates. In a nutshell, the S_{eq} of the hydrogel was mainly governed by the solvation of the polymer chain and the filling of the pores by the solvent. One could envisage that a higher porosity would result in a high swelling ratio because of the larger size pore formed by the polymer chains in the hydrogel network. The larger pore size caused a loose structure, which greatly improved the water-absorbing capacity of the hydrogel because the large pores allowed a greater volume of void space to be filled by the solvent. The increasing pore size and porosity of the hydrogel permitted a greater access of water molecules to the hydrogel; this further expanded the network of hydrogels. Hence, SC had the lowest S_{eq} value because of its dense and less porous structure [Figure 2(a)]. Furthermore, all of the $S_{eq(exp)}$ values were in good agreement with the respective $S_{eq(calc)}$ values, as shown in Table II.

Oscillatory Swelling–Deswelling of the Hydrogels

The oscillatory swelling–deswelling of the hydrogels was investigated by the alternation of the ionic strength of the PBS solutions (pH 7.4) between 0.15 and 0.05 *M*. As shown in Figure 9, the semi-IPN PAAc/PASP hydrogels (IPN 37–25 and IPN 37–F20) demonstrated the best swelling–deswelling reversibility in response to the change in the ionic strength of the PBS solution. The excellent swelling–deswelling reversibility of the semi-IPN PAAc/PASP hydrogel was due to the incorporation of PASP in the PAAc hydrogel structure.

The durations required by IPN 37–F20 to swell and deswell to its equilibrium state were 12 and 21 min, respectively. On the contrary, the durations of equilibrium swelling and deswelling for IPN 37–F20 were 15 and 24 min, respectively. Hence, we concluded that the swelling–deswelling processes of IPN 37–F20 were relatively quicker than those of IPN 37–25 in simulated physiological fluid. We believe the porous structure of the semi-IPN PAAc/PASP hydrogels to be the reason behind the relatively fast expansion–shrinking of the freeze-polymerized hydrogels in the physiological fluid.

Among the five types of hydrogels, IPN 37–F20 demonstrated the best ionic-strength sensitivity because of its largest difference

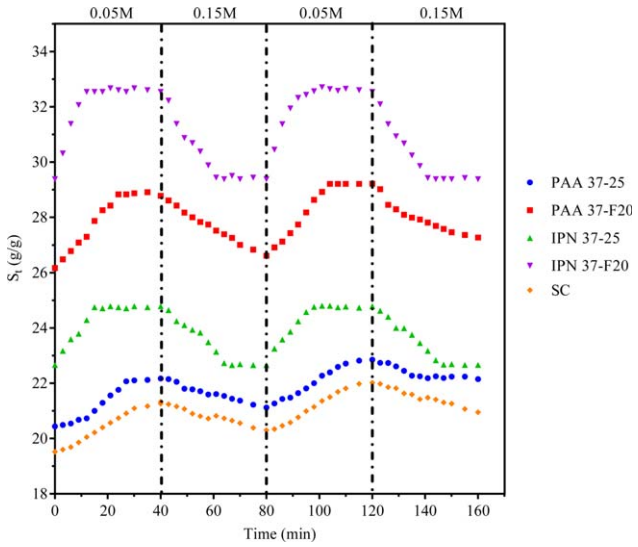

Figure 9. Time-dependent ionic-strength response of the PAAc and semi-IPN PAAc/PASP hydrogels incubated in a PBS solution at pH 7.4. The ionic strength of the PBS solution was cycled between 0.05 and 0.15 *M* every 40 min for a total of 160 min. [Color figure can be viewed in the online issue, which is available at wileyonlinelibrary.com.]

in equilibrium swelling and deswelling states. The PAAc hydrogels (i.e., SC, PAA 37–25, and PAA 37–F20) exhibited poor ionic-strength reversibility. Moreover, the swelling ratio of the PAAc hydrogel increased gradually with the increasing number of oscillatory cycles. This trend could have been due to the relatively slow deswelling rate of the PAAc hydrogel as compared to its swelling rate.

Overall, the excellent response of IPN 37–F20 toward the change in the ionic strength makes them suitable for use in applications demanding the rapid swelling–deswelling of hydrogels, for example, in the controlled release of drugs from the matrix or as components in biosensors.[12–14]

CONCLUSIONS

In this study, a two-step free-radical polymerization was applied to the synthesis of semi-IPN PAAc/PASP hydrogels with the aim of improving their ionic-strength responsivity. The swelling behavior of the hydrogels was perfectly fitted to Schott's second-order swelling kinetics model. Overall, the swelling and deswelling rates of the PAAc hydrogels were improved by the freezing polymerization step and the incorporation of PASP into the hydrogel structure. IPN 37–F20 is a good candidate hydrogel for use in practical applications because of its excellent sensitivity and reversibility toward ionic strength. The semi-IPN PAAc/PASP hydrogel is a promising material for use in biosensors, biomedicine, and pharmaceuticals.

ACKNOWLEDGMENTS

One of the authors (S.L.L.) was supported by the School of Engineering and Advanced Engineering Platform (Monash University Malaysia) through a Higher Degree Research Scholarship.

REFERENCES

1. Zhao, Y.; Tan, T.; Kinoshita, T. *J. Polym. Sci. Part B: Polym. Phys.* **2010**, *48*, 666.
2. Schmaljohann, D. *Drug Delivery Rev.* **2006**, *58*, 1655.
3. Hoffman, A. S.; Stayton, P. S.; Bulmus, V.; Chen, G.; Chen, J.; Cheung, C.; Chilkoti, A. *J. Biomed. Mater. Res.* **2000**, *52*, 577.
4. Hoffman, A. S. *Adv. Drug Delivery Rev.* **2013**, *65*, 10.
5. Jin, S.; Liu, M.; Zhang, F.; Chen, S.; Niu, A. *Polymer* **2006**, *47*, 1526.
6. Tanaka, T.; Nishio, I.; Sun, S.-T.; Ueno-Nishio, S. *Science* **1982**, *218*, 467.
7. Bae, Y. H.; Okano, T.; Hsu, R.; Kim, S. W. *Makromol. Chem. Rapid Commun.* **1987**, *8*, 481.
8. Lin, G.; Chang, S.; Kuo, C.-H.; Magda, J.; Solzbacher, F. *Sens. Actuators B* **2009**, *136*, 186.
9. Agarwal, A.; Unfer, R. C.; Mallapragada, S. K. *Biomaterials* **2008**, *29*, 607.
10. Dadsetan, M.; Liu, Z.; Pumberger, M.; Giraldo, C. V.; Ruesink, T.; Lu, L.; Yaszemski, M. J. *Biomaterials* **2010**, *31*, 8051.
11. Qian, Y.-C.; Chen, P.-C.; Zhu, X.-Y.; Huang, X.-J. *RSC Adv.* **2015**, *5*, 44031.
12. Holtz, J. H.; Asher, S. A. *Nature* **1997**, *389*, 829.
13. Asher, S. A.; Alexeev, V. L.; Goponenko, A. V.; Sharma, A. C.; Lednev, I. K.; Wilcox, C. S.; Finegold, D. N. J. *Am. Chem. Soc.* **2003**, *125*, 3322.
14. Alexeev, V. L.; Sharma, A. C.; Goponenko, A. V.; Das, S.; Lednev, I. K.; Wilcox, C. S.; Finegold, D. N.; Asher, S. A. *Anal. Chem.* **2003**, *75*, 2316.
15. Kim, S. J.; Lee, K. J.; Kim, I. Y.; Lee, Y. M.; Kim, S. I. *J. Appl. Polym. Sci.* **2003**, *90*, 3310.
16. Zhao, Y.; Kang, J.; Tan, T. *Polymer* **2006**, *47*, 7702.
17. Philippova, O. E.; Hourdet, D.; Audebert, R.; Khokhlov, A. R. *Macromolecules* **1997**, *30*, 8278.
18. Yaung, J. F.; Kwei, T. *J. Appl. Polym. Sci.* **1998**, *69*, 921.
19. Karbarz, M.; Hyk, W.; Stojek, Z.; *Electrochem. Commun.* **2009**, *11*, 1217.
20. Gehrke, S. H. *Adv. Polym. Sci.* **1993**, *110*, 81.
21. Liu, C.; Gan, X.; Chen, Y. *Starch* **2011**, *63*, 503.
22. Xue, W.; Champ, S.; Huglin, M. B.; Jones, T. G. *Eur. Polym. J.* **2004**, *40*, 467.
23. Liu, H.; Liu, M.; Huang, J.; Ma, L.; Chen, J. *Polym. Adv. Technol.* **2009**, *20*, 1152.
24. Pourjavadi, A.; Harzandi, A. M.; Hosseinzadeh, H. *Eur. Polym. J.* **2004**, *40*, 1363.
25. Foreman, J.; Lundgren, C.; Gill, P. Tech. *Pap. Annu. Tech. Conf. Soc. Plast. Eng.* **1993**, 3025.
26. Schott, H. *J. Macromol. Sci. Phys.* **1992**, *31*, 1.
27. Yin, Y.; Yang, Y.; Xu, H. *J. Polym. Sci. Part B: Polym. Phys.* **2001**, *39*, 3128.
28. Saraydın, D.; Işıkver, Y.; Karadağ, E.; Sahiner, N.; Güven, O. *Nucl. Instrum. Methods Phys. Res. Sect. B* **2002**, *187*, 340.
29. Karadağ, E.; Üzüm, Ö. B.; Saraydin, D.; Güven, O. *Int. J. Pharm.* **2005**, *301*, 102.
30. Tomida, M.; Yabe, M.; Arakawa, Y. *Polymer* **1997**, *38*, 2791.
31. Leibler, L. *Macromolecules* **1980**, *13*, 1602.
32. Zhang, X.-Z.; Yang, Y.-Y.; Wang, F.-J.; Chung, T.-S. *Langmuir* **2002**, *18*, 2013.
33. Nakamoto, C.; Motonaga, T.; Shibayama, M. *Macromolecules* **2001**, *34*, 911.
34. Alvarez-Lorenzo, C.; Guney, O.; Oya, T.; Sakai, Y.; Kobayashi, M.; Enoki, T.; Takeoka, Y.; Ishibashi, T.; Kuroda, K.; Tanaka, K. *Macromolecules* **2000**, *33*, 8693.
35. Xue, W.; Hamley, I. W.; Huglin, M. B. *Polymer* **2002**, *43*, 5181.
36. Qu, X.; Wirsén, A.; Albertsson, A. C. *J. Appl. Polym. Sci.* **1999**, *74*, 3186.
37. Mandal, B.; Ray, S. K. *Carbohydr. Polym.* **2013**, *98*, 257.
38. Zhang, X.-Z.; Zhuo, R.-X. *Macromol. Chem. Phys.* **1999**, *200*, 2602.
39. Liu, M.; Su, H.; Tan, T. *Carbohydr. Polym.* **2012**, *87*, 2425.